Supporting Information

N-Nitrosodimethylamine (NDMA) Degradation by the UV/peroxodisulfate Process

Inmaculada Velo-Gala[1], María J. Farré[1], Jelena Radjenovic[1,2], Wolfgang Gernjak [1,2,*].

(1) Catalan Institute for Water Research (ICRA). Emili Grahit 101, 17003 Girona, Spain.

(2) Catalan Institute for Research and Advanced Studies (ICREA), Passeig Lluís Companys 23, 08010 Barcelona, Spain.

* corresponding author: wgernjak@icra.cat, phone: +34-972-183380

Contents of supporting information:

Text S1. Method for N-nitrosodimethylamine determination in aqueous solution

The procedure for NDMA analysis [1] was modified from the headspace method proposed by Grebel et al. (2006) [2]. GC-QqQ analysis was performed by Trace GC Ultra gas chromatograph equipped with a TriPlus™ autosampler coupled to a TSQ Quantum triple quadrupole mass spectrometer system (Thermo Fisher Scientific). 5 mL of the sample were placed in an amber vial containing 1.8 g of sodium chloride. Finally 100 µL of d_6NDMA 10 µg/L were added as internal standard. Carboxen/polydimethylsiloxane (CAR/PDMS) fibres from Supelco were selected for the extraction. The fibres were first conditioned to remove contaminants in the GC inlet prior to use as recommended by the manufacturer. Extraction was achieved by heating up and stirring the sample at 80ºC during 45 min. The fibre was exposed to the head-space generated in the sample vial. Once extraction and pre-concentration steps were achieved, the fibre was pulled out of the sample vial and injected into the GC. Desorption was conducted at 250ºC during 4 minutes. Blanks were run periodically during the analysis to confirm the absence of carry over. Chromatographic separation was performed using a Trace GOLD TG-5SILMS from Thermo Fisher Scientific (30m x 0.25mm x 0.25µm). The injector was operated in splitless mode. The oven temperature program was as follows: 50ºC hold for 3 minutes, ramp to 180ºC at 25ºC/min, hold for 0.5 minutes, ramp to 230ºC at 40ºC/min, and finally hold for 1 minute. The limit of quantification (LOQ) was 20 ng/L, which allows a good observation of the degradation kinetics, which were carried out with an initial concentration of 500 ng/L.

The peak area of a standard prepared at 1000 ng/L in dichloromethane and injected directly was compared to the peak area of a standard prepared at 1000 ng/L in water and extracted with SPME. We observed that the area of the standard extracted with SPME was 100 times higher than the standard prepared in dichloromethane and injected directly, meaning that there is a factor of 100 enrichment during SPME. When calculating the recovery using quality control standards and using the calibration curve, we observed recoveries between 90-95%.

Mass spectrometric ionization was carried out in electron impact (EI) ionization mode with and EI voltage of 70 eV and a source temperature of 250ºC. Detection was performed in Selected Reaction Monitoring (SRM) mode. NDMA was monitored by using the m/z 74 parent ion and 42 and 43 daughter ions as quantification and qualification transitions, respectively. The internal standard d_6NDMA was quantified by using the m/z 80 parent ion and 46 daughter ion. Acquired data were processed by TracerFinder EFS 3.1 software.

Text S2. Evaluation of fluence and fluence-based rate constants

The UV-fluence and the incident photon irradiance of the polychromatic lamp were determined as previously described by Bolton et. al [3] in the range of **200-300 nm**. This range was considered due as it contains the main absorption band of NDMA (peak at 227 nm). The value of average fluence rate was determined experimentally from the incident photon irradiance in the centre of the reactor and correction factors such as Petri Factor (PF), Reflection Factor (RF), and Water Factor (WF) [3].

The data of the **lamp irradiance** (W cm^{-2}) that was applied to determine the different parameters was taken at the center of the beam at the water surface. In addition, radiometer measurements were taken across the surface area at the level of the water surface in the Petri dish in a manner that allows the calculation of the average irradiance over that surface area. With these results, the **PF** was calculated by dividing the average irradiance across the water surface by the measure in the center of the Petri dish. The PF value was 0.97 and the incident photon irradiance was 4.16 W m^{-2}. The **WF** represents the absorbance of the water and is calculated from an integration of Beer's Law from the top to the bottom of the solution [3]. The applied data of **RF** for water at a given wavelength was taken from the bibliography [3, 4]. Analyzing the photon fluence-degradation of NDMA, an additional factor is required as a ***NDMA-factor***, which defined the photolysis effectiveness of photons of a certain wavelength relative to those at 254 nm. With these data, the **average photon irradiance** and the **equivalent average irradiance** at 254 nm were calculated for each experiment using the Excel spreadsheet provided in their supplementary information by Bolton et. al [3]. The evaluation of **UV fluence** (J m^{-2}) was done by multiplying the exposure time (second) by the equivalent average irradiance at 254 nm (W m^{-2}) of each experiment conditions. According with this setting, the equivalent average irradiance at 254 nm (table S1, exp. 5) was 5.25 W m^{-2}. On the other hand, the uncorrected average photon irradiance between 200 and 300 nm was 3.54 W cm^{-2}. These values increased less than 1% when the $K_2S_2O_8$ concentration was decreased to zero.

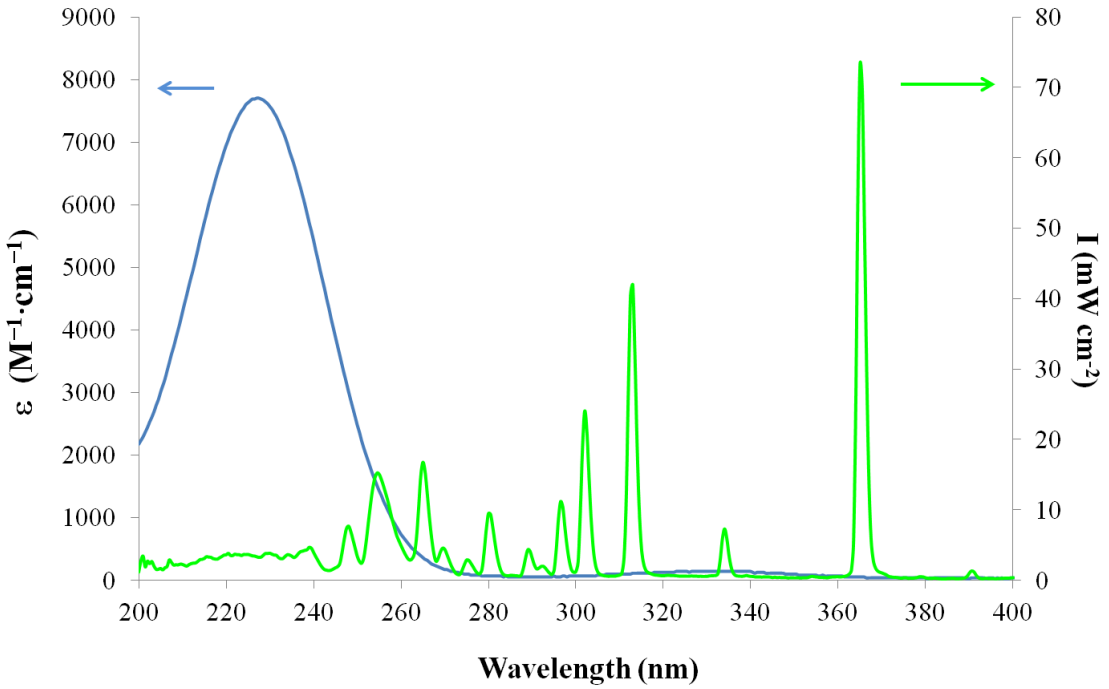

Figure S1. Emission spectrum of UV Medium Pressure Lamp and absorption spectra of NDMA

Text S3. Results supporting the description of experimental reaction kinetics

Table S1. Results obtained for NDMA photodegradation processes. $[NDMA]_0 = 6.75x10^{-9}$ M. pH = 6

Nº exp.	UV-MP	$S_2O_8^{2-}$ (μM)	IC (mM)	Cl^- (mM)	SO_4^{2-} (mM)	NDMA Degradation (%) 4.7×10^3 J m^{-2} (15 min)	*$k_{obs} \times 10^{-4}$ (m^2 J^{-1})	R square
1	✓	0	0	0	0	73.1	2.56 ± 0.32	0.97
2	×	33.6	0	0	0	13.1	(0.83 ± 0.06) $\times 10^{-2}$ min^{-1}	0.99
3	✓	6.72	0	0	0	77.5	3.18 ± 0.95	0.95
4	✓	20.2	0	0	0	95.2	6.68 ± 0.96	0.99
5	✓	33.6	0	0	0	100	9.30 ± 1.92	0.98
6	✓	33.6	0.25	0	0	83.5	3.89 ± 0.86	0.97
7	✓	33.6	0.5	0	0	78.8	3.29 ± 0.68	0.97
8	✓	33.6	0.75	0	0	73.8	2.72 ± 0.51	0.98
9	✓	33.6	1	0	0	64.8	2.34 ± 0.53	0.97
10	✓	33.6	0	0.25	0	90.4	4.90 ± 0.88	0.98
11	✓	33.6	0	0.5	0	76.5	3.11 ± 0.82	0.96
12	✓	33.6	0	0.75	0	80.0	3.58 ± 0.83	0.97
13	✓	33.6	0	1	0	77.5	3.36 ± 0.85	0.96
14	✓	33.6	0	0	1	97.4	7.71 ± 0.91	0.99
15	✓	33.6	1	1	1	75.3	2.93 ± 0.65	0.97
16	✓	33.6	0.5	0.5	0.5	79.9	3.36 ± 0.24	0.99

* The fluence-based rate constants (k_{obs}, m^2 J^{-1}) were determined from the first-order plot of the natural logarithm of the normalized NDMA concentration versus the UV-fluence. The data were fitted by a first-order kinetic and the slopes of the lines represent the observed fluence-based rate constants k_{obs}. The error values for k_{obs} correspond to the 95% confidence interval of the linear fit.

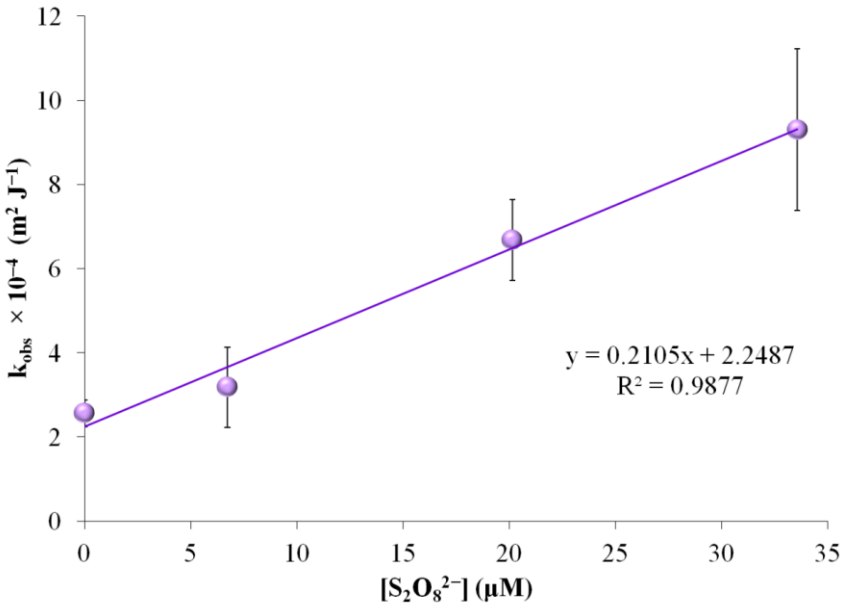

Figure S2. Linear increase in the NDMA degradation rate constant value as a function of the $S_2O_8^{2-}$ concentration in MP-UV processes.

Text S4. Kinetic modelling approach

The kinetic modelling was conducted using the modelling package Kintecus® v6.70. In the course of the kinetic modelling study we estimated the reaction rate constant for the reactions of NDMA with the sulfate, carbonate and dichloride anion radicals based on our experimental data, changing the values of the estimated constants and studying the impact on the evolution of the system.

The experiments 1, 3, 4 and 5 (table S1) were used for the fit of the estimation of the reaction rate constant between NDMA and the sulfate radical. In the case of the rate constant with the carbonate radical, the fit was made using the previously fitted rate constant for NDMA and sulfate radical to fit the results of the experiments num. 6 – 9, 15 and 16 (table S1) by adjusting the reaction rate of the carbonate radical with NDMA. Finally, to obtain the k value of NDMA with the dichloride anion radical, the adjustment was made using experiments 10 – 16.

Table S2. Principal reactions in kinetic model

Reaction	Rate constant	No. Ref.
$S_2O_8^{2-} + h\nu \rightarrow 2SO_4^{\bullet-}$	$\Phi = 0.70$	(1a) [5]
NDMA + $h\nu \rightarrow$ product	$\Phi = 0.30$	(1b) [6]
$SO_4^{\bullet-} + SO_4^{\bullet-} \rightarrow S_2O_8^{2-}$	$k = 8.10 \times 10^8\ M^{-1}\ s^{-1}$	(2) [7]
$SO_4^{\bullet-} + S_2O_8^{2-} \rightarrow SO_4^{2-} + S_2O_8^{\bullet-}$	$k = 1.50 \times 10^5\ M^{-1}\ s^{-1}$	(3) [7]
$SO_4^{\bullet-} + H_2O \rightarrow SO_4^{2-} + H^+ + {}^{\bullet}OH$	$k = 0.002\ M^{-1}\ s^{-1}$	(4) [8]
${}^{\bullet}OH + H_2O_2 \rightarrow HO_2^{\bullet} + H_2O$	$k = 2.70 \times 10^7\ M^{-1}\ s^{-1}$	(5) [9]
${}^{\bullet}OH + {}^{\bullet}OH \rightarrow H_2O_2$	$k = 5.50 \times 10^9\ M^{-1}\ s^{-1}$	(6) [9]
$SO_4^{\bullet-} + {}^{\bullet}OH \rightarrow HSO_4^- + \frac{1}{2}O_2$	$k = 1.00 \times 10^{10}\ M^{-1}\ s^{-1}$	(7) [10]
$S_2O_8^{2-} + {}^{\bullet}OH \rightarrow HSO_4^- + SO_4^{\bullet-} + \frac{1}{2}O_2$	$k = 1.20 \times 10^7\ M^{-1}\ s^{-1}$	(8) [11]
NDMA + $SO_4^{\bullet-} \rightarrow$ products	$k = 1.20 \times 10^7\ M^{-1}\ s^{-1}$	(9) this study
NDMA + ${}^{\bullet}OH \rightarrow$ products	$k = 3.80 \times 10^8\ M^{-1}\ s^{-1}$	(10) [12]
NDMA + $CO_3^{\bullet-} \rightarrow$ products	$k = 2.00 \times 10^4\ M^{-1}\ s^{-1}$	(11) this study
NDMA + $Cl_2^{\bullet-} \rightarrow$ products	$k = 3.00 \times 10^5\ M^{-1}\ s^{-1}$	(12) this study
Reactions added to reactions 1-8 for the estimation of k (NDMA + $SO_4^{\bullet-}$) (reaction 9)		
$HO_2^{\bullet} + H_2O_2 \rightarrow O_2 + {}^{\bullet}OH + H_2O$	$k = 3.00\ M^{-1}\ s^{-1}$	(13) [9]
$HO_2^{\bullet} + HO_2^{\bullet} \rightarrow O_2 + H_2O_2$	$k = 8.30 \times 10^9\ M^{-1}\ s^{-1}$	(14) [9]
${}^{\bullet}OH + HO_2^{\bullet} \rightarrow O_2 + H_2O$	$k = 6.60 \times 10^9\ M^{-1}\ s^{-1}$	(15) [9]
$SO_4^{\bullet-} + OH^- \rightarrow SO_4^- + {}^{\bullet}OH$	$k = 7.70 \times 10^7\ M^{-1}\ s^{-1}$	(16) [13]
$S_2O_8^{\bullet-} + OH^- \rightarrow S_2O_8^{2-} + {}^{\bullet}OH$	$k = 6.50 \times 10^7\ M^{-1}\ s^{-1}$	(17) [13]
$H^+ + OH^- \rightarrow H_2O$	$k = 1.00 \times 10^{11}\ M^{-1}\ s^{-1}$	(18) [14]
MeOH + $SO_4^{\bullet-} \rightarrow$ products	$k = 1.00 \times 10^7\ M^{-1}\ s^{-1}$	(19) [15]
MeOH + ${}^{\bullet}OH \rightarrow$ products	$k = 9.70 \times 10^8\ M^{-1}\ s^{-1}$	(20) [9]

Reaction	Rate constant	No. [Ref.]
Additional reactions added for the estimation of k (NDMA + $CO_3^{\bullet-}$) (reaction 11)		
$SO_4^{\bullet-} + HCO_3^- \rightarrow CO_3^{\bullet} + H^+ + SO_4^{2-}$	$k = 2.80 \times 10^6\ M^{-1}\ s^{-1}$	(21) [16]
$SO_4^{\bullet-} + CO_3^{2-} \rightarrow CO_3^{\bullet-} + SO_4^{2-}$	$k = 2.50 - 6.10 \times 10^6\ M^{-1}\ s^{-1}$	(22) [16]
$CO_3^{\bullet-} + {}^{\bullet}OH \rightarrow$ products	$k = 3.00 \times 10^9\ M^{-1}\ s^{-1}$	(23) [17]
$H_2CO_3 + {}^{\bullet}OH \rightarrow$ products $+ H_2O + H^+$	$k = 1.00 \times 10^6\ M^{-1}\ s^{-1}$	(24)[9]
$CO_3^{\bullet-} + S_2O_8^{2-} \rightarrow CO_3^{2-} + S_2O_8^{\bullet-}$	$k = 3.00 \times 10^4\ M^{-1}\ s^{-1}$	(25) [14]
$HCO_3^- + Cl^{\bullet} \rightarrow H_2O + CO_3^{\bullet-}$	$k = 2.40 \times 10^9\ M^{-1}\ s^{-1}$	(26) [18]
$CO_3^{2-} + Cl^{\bullet} \rightarrow OH^- + CO_3^{\bullet-}$	$k = 5.00 \times 10^8\ M^{-1}\ s^{-1}$	(27) [18]
$HCO_3^- + Cl_2^{\bullet-} \rightarrow 2Cl^- + H^+ + CO_3^{\bullet-}$	$k = 8.00 \times 10^7\ M^{-1}\ s^{-1}$	(28) [19]
$CO_3^{2-} + Cl_2^{\bullet-} \rightarrow 2Cl^- + CO_3^{\bullet-}$	$k = 1.60 \times 10^8\ M^{-1}\ s^{-1}$	(29) [19]
$CO_3^{2-} + {}^{\bullet}OH \rightarrow CO_3^{\bullet-} + OH^-$	$k = 3.90 \times 10^8\ M^{-1}\ s^{-1}$	(30) [9]
$HCO_3^- + {}^{\bullet}OH \rightarrow CO_3^{\bullet-} + H_2O$	$k = 8.60 \times 10^6\ M^{-1}\ s^{-1}$	(31) [9]
$CO_3^{2-} + H^+ \rightarrow HCO_3^-$	$k = 5.00 \times 10^{10}\ M^{-1}\ s^-$	(32) [14]
Additional reactions added for the estimation of k (NDMA + $Cl_2^{\bullet-}$) (reaction 12)		
$SO_4^{\bullet-} + Cl^- \rightarrow Cl^{\bullet} + SO_4^{2-}$	$k = 3.00 \times 10^8\ M^{-1}\ s^{-1}$	(33) [10]
$Cl^{\bullet} + Cl^{\bullet} \rightarrow Cl_2$	$k = 8.80 \times 10^7\ M^{-1}\ s^{-1}$	(34) [20]
$Cl^- + Cl^{\bullet} \leftrightarrow Cl_2^{\bullet-}$	$k = 6.50 \times 10^9\ M^{-1}\ s^{-1}$	(35) [21]
$Cl_2^{\bullet-} + Cl_2^{\bullet-} \rightarrow Cl_2 + 2Cl^-$	$k = 9.00 \times 10^8\ M^{-1}\ s^{-1}$	(36) [22]
$Cl_2^{\bullet-} + Cl^{\bullet} \rightarrow Cl_2 + Cl^-$	$k = 2.10 \times 10^9\ M^{-1}\ s^{-1}$	(37) [22]
$Cl^{\bullet} + S_2O_8^{2-} \rightarrow$ products	$k = 8.80 \times 10^6\ M^{-1}\ s^{-1}$	(38) [23]
$Cl_2^{\bullet-} + S_2O_8^{2-} \rightarrow$ products	$k = 1.00 \times 10^4\ M^{-1}\ s^{-1}$	(39) [23]
${}^{\bullet}OH + Cl^- \rightarrow ClOH^{\bullet-}$	$k = 4.30 \times 10^9\ M^{-1}\ s^{-1}$	(40) [24]
$ClOH^{\bullet-} \rightarrow {}^{\bullet}OH + Cl^-$	$k = 6.10 \times 10^9\ M^{-1}\ s^{-1}$	(41) [21]
$Cl_2^{\bullet-} + {}^{\bullet}OH \rightarrow HOCl + Cl^-$	$k = 1.00 \times 10^9\ M^{-1}\ s^{-1}$	(42) [25]
$Cl_2^{\bullet-} + HO_2^{\bullet} \rightarrow O_2 + 2Cl^- + H^+$	$k = 3.00 \times 10^9\ M^{-1}\ s^{-1}$	(43) [25]
$Cl^{\bullet} + HOCl \rightarrow ClO^{\bullet} + Cl^- + H^+$	$k = 3.00 \times 10^9\ M^{-1}\ s^{-1}$	(44) [26]
$Cl^{\bullet} + + H_2O_2 \rightarrow HO_2^{\bullet} + Cl^- + H^+$	$k = 2.00 \times 10^9\ M^{-1}\ s^{-1}$	(45) [22]
$ClOH^{\bullet-} + Cl^- \rightarrow Cl_2^{\bullet-} + OH^-$	$k = 2.10 \times 10^{10}\ M^{-1}\ s^{-1}$	(46) [27]
$ClOH^{\bullet-} + H^+ \rightarrow Cl^{\bullet} + H_2O$	$k = 1.00 \times 10^4\ M^{-1}\ s^{-1}$	(47) [24]
$HOCl + {}^{\bullet}OH \rightarrow ClO^{\bullet} + H_2O$	$k = 2.00 \times 10^9\ M^{-1}\ s^{-1}$	(48) [19]
$SO_4^{2-} + Cl^{\bullet} \rightarrow SO_4^{\bullet-} + Cl^-$	$k = 2.50 \times 10^8\ M^{-1}\ s^{-1}$	(49) [10]
$MeOH + Cl^{\bullet} \rightarrow$ products	$k = 1.00 \times 10^9\ M^{-1}\ s^{-1}$	(50) [28]

Text S5. Comparison of the results of kinetic modelling and experimental observation

Incident photon irradiance is I = 4.16 W m^{-2} and error bars represent the mean deviation of experimental duplicate values in all subsequent figures.

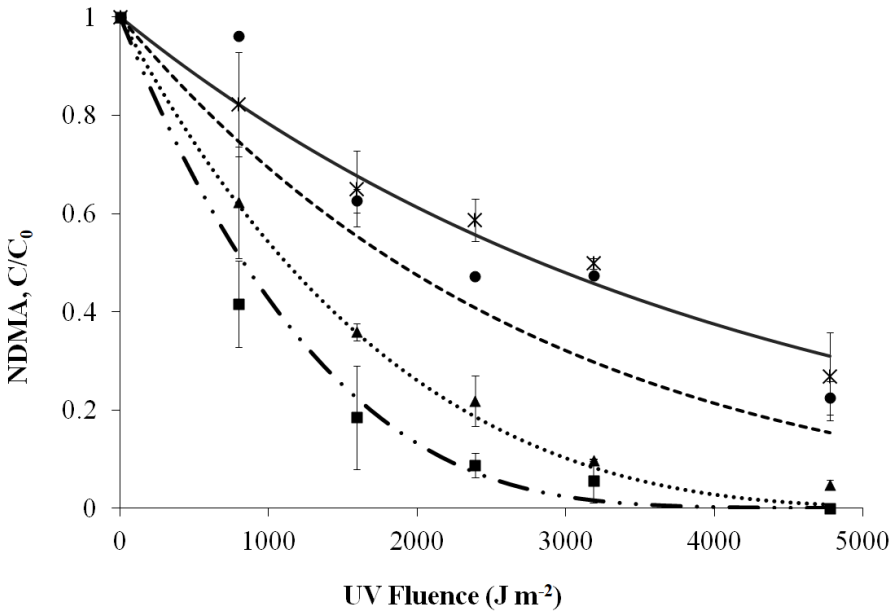

Figure S3. Kinetic modelling of the impact of the $K_2S_2O_8$ concentration in the NDMA degradation during MP-UV irradiation (table S1, exp. 1, 3 – 5). $[S_2O_8^{2-}]_0$ (μM) = 0 (—✳—); 6.72 (--●--); 20.2 (··▲··); 33.6 (–··–■–··–). $[NDMA]_0 = 6.75\times10^{-9}$ M. pH = 6.

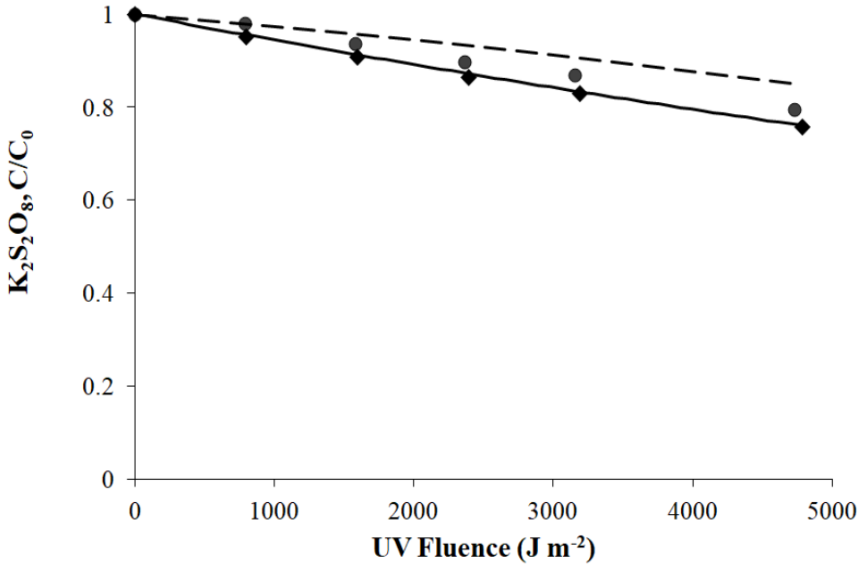

Figure S4. Kinetic modelling of the $K_2S_2O_8$ concentration in the MP-UV system with 33.6 μM as initial concentration of the oxidant, in HPLC water (--●--) and water with 1 mM of sulfate, bicarbonate and chloride anions (—◆—) (table S1, exp. 5 and 15).

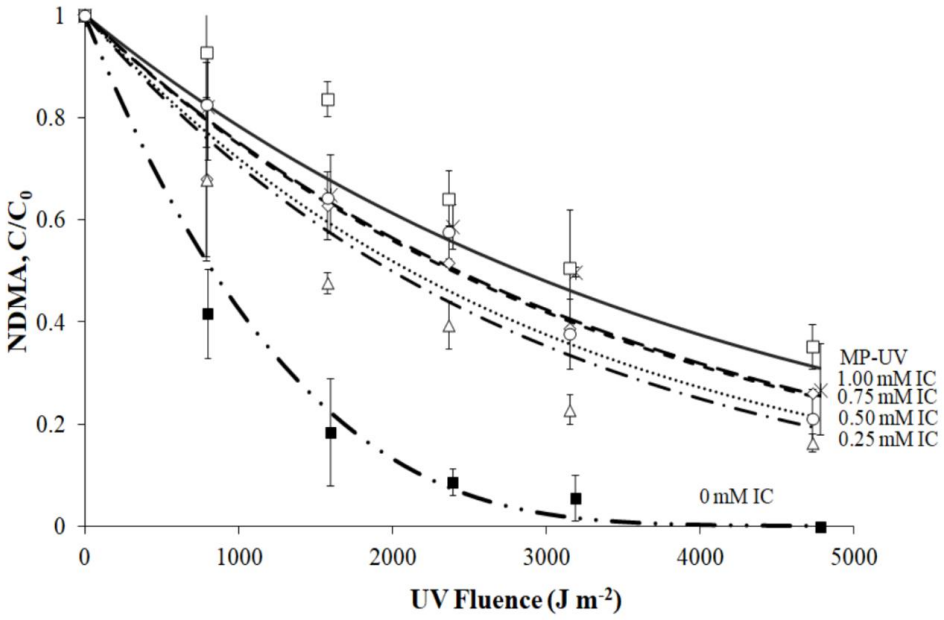

Figure S5. Kinetic modelling of the effect of the IC concentration on the NDMA degradation during MP-UV irradiation with 33.6 μM of $S_2O_8^{2-}$ initial concentration (table S1, exp. 1, 5 – 9). Degradation processes: UV (—✳—); UV/$S_2O_8^{2-}$ with [IC] = 0 mM (–··–■–··–), 0.25 mM (–·–△–·–), 0.5 mM (··○··), 0.75 mM (--◇--), 1 mM (– –□– –). $[NDMA]_0 = 6.75\times10^{-9}$ M. pH = 6.

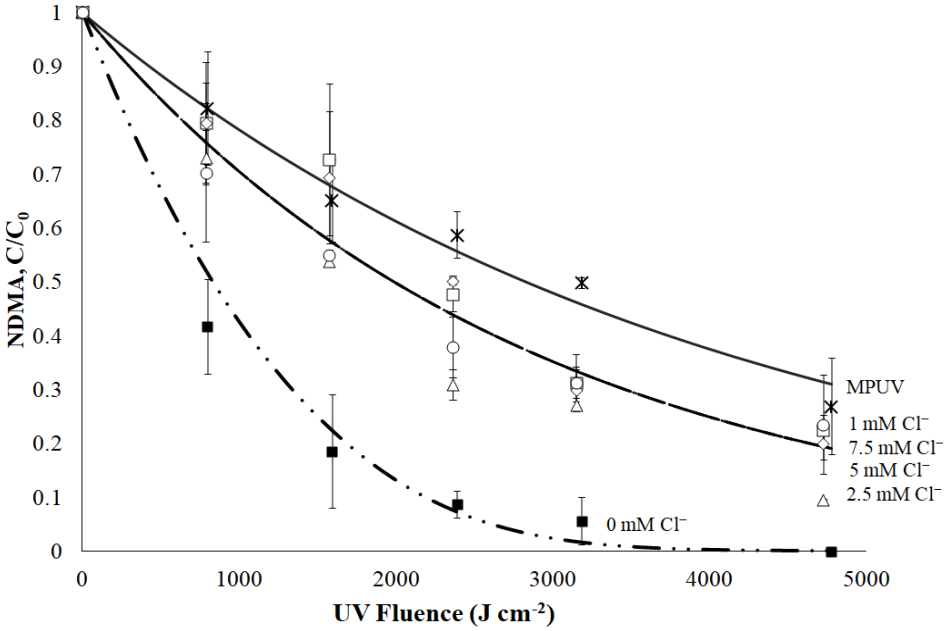

Figure S6. Kinetic modelling of the effect of the Cl^- concentration on the NDMA degradation during MP-UV irradiation with 33.6 μM of $S_2O_8^{2-}$ initial concentration (table S1, exp. 1, 5, 10 – 13). Degradation processes: UV (—✳—); UV/$S_2O_8^{2-}$ with [Cl^-] = 0 mM (–··–■–··–), 0.25 mM (–·–△–·–), 0.5 mM (··○··), 0.75 mM (--◇--), 1 mM (– –□– –). $[NDMA]_0$ = 6.75×10^{-9} M. pH = 6.

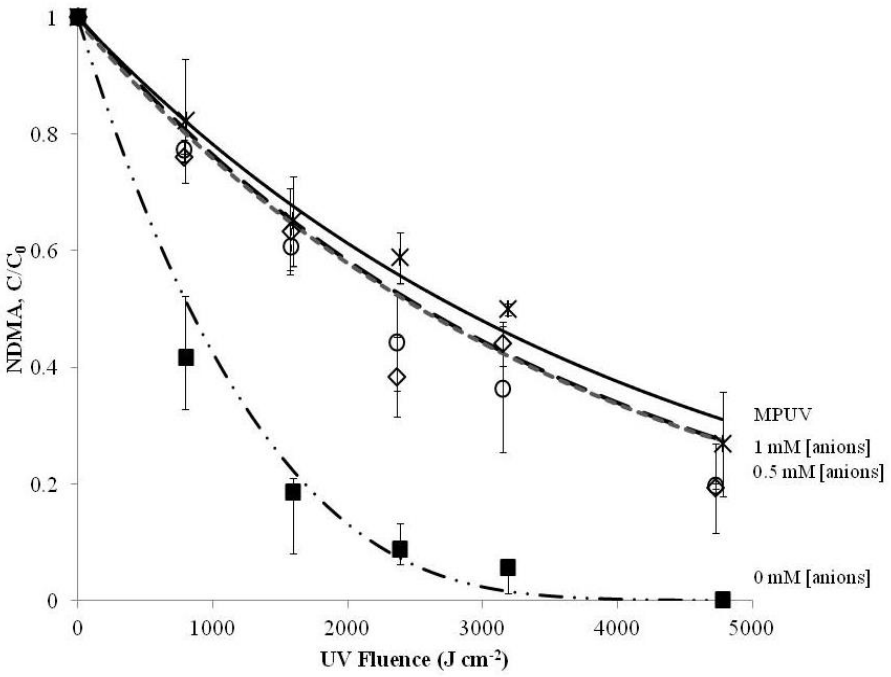

Figure S7. Kinetic modelling of the effect of the simultaneous presence of IC, SO_4^{2-}, and Cl^-on the NDMA degradation during MP-UV irradiance with 33.6 μM of $S_2O_8^{2-}$ initial concentration (table S1, exp. 1, 5, 15, 16). Degradation processes: UV (—✳—); UV/$S_2O_8^{2-}$ with [anions] = 0 mM each (–···–■–···–), 0.5 mM each (--○--), 1mM each (– –◇– –). $[NDMA]_0 = 6.75\times10^{-9}$ M. pH = 6.

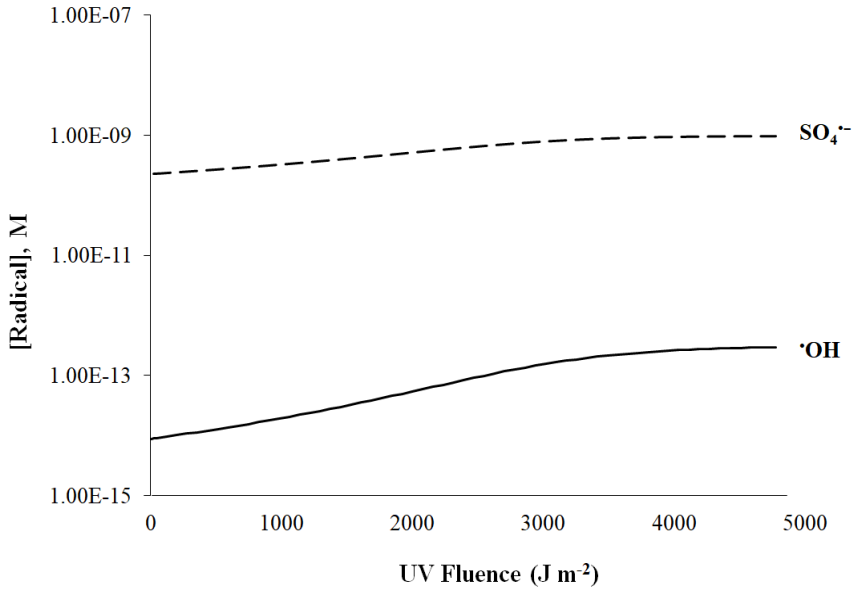

Figure S8. Oxidant species distribution obtained by kinetic modelling in the UV/$K_2S_2O_8$ system in HPLC water during MP-UV irradiation. $[S_2O_8^{2-}]_0$= 33.6 μM.

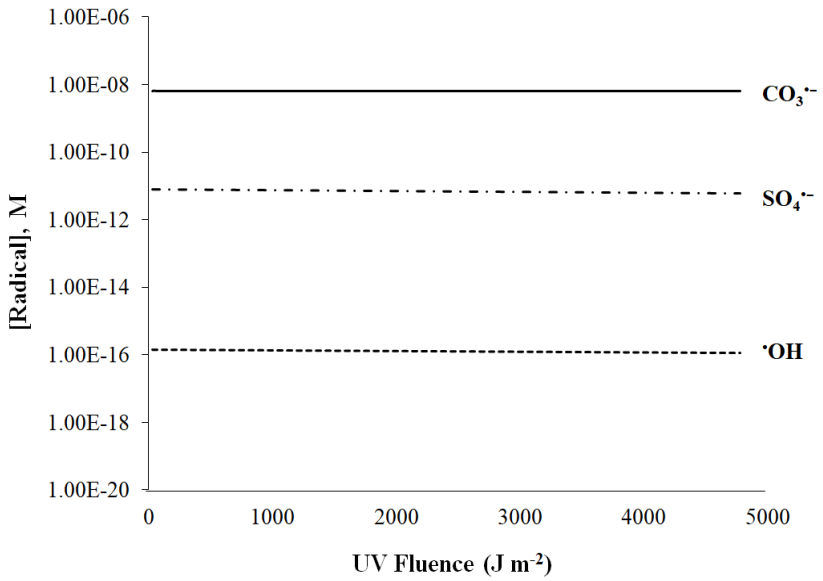

Figure S9. Oxidant species distribution obtained by kinetic modelling in the UV/$K_2S_2O_8$ system in water with 1mM of IC during MP-UV irradiation. $[S_2O_8^{2-}]_0$= 33.6 µM.

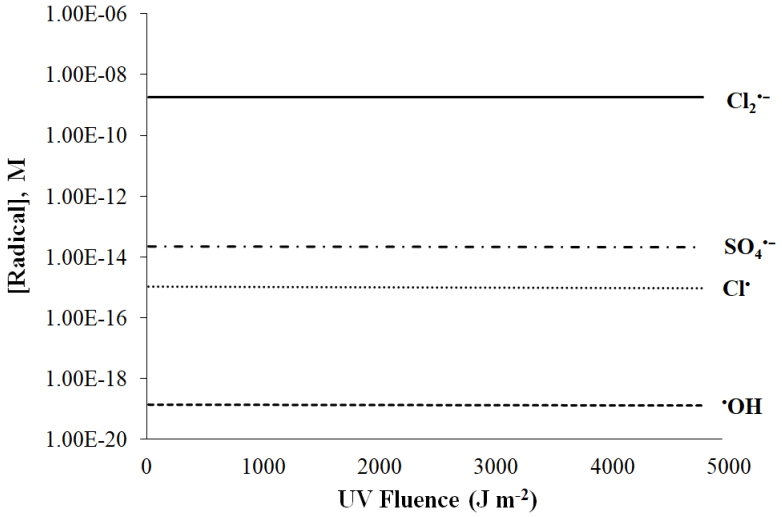

Figure S10. Oxidant species distribution obtained by kinetic modelling in the UV/$K_2S_2O_8$ system in water with 1mM of Cl^- during MP-UV irradiation. $[S_2O_8^{2-}]_0$= 33.6 µM.

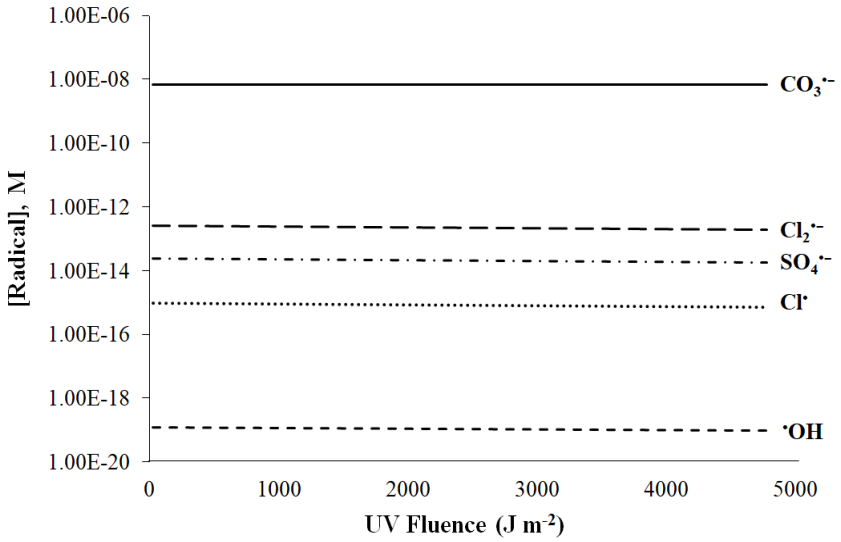

Figure S11. Oxidant species distribution during MP-UV irradiation obtained by kinetic modelling in the UV/$K_2S_2O_8$ system in water with simultaneous presence of IC, SO_4^{2-}, and Cl^- at 1mM concentration of each of them. $[S_2O_8^{2-}]_0$= 33.6 µM.

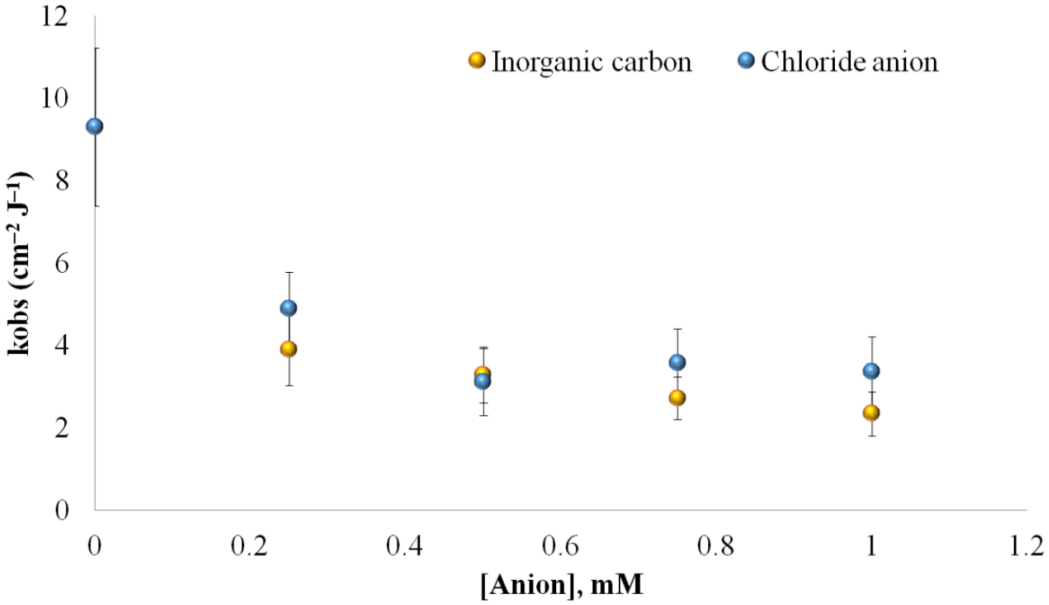

Figure S12. Effect of concentration of chloride and IC on the rate of NDMA degradation by UV/$K_2S_2O_8$ during MP-UV irradiation. $[S_2O_8^{2-}]_0$ = 33.6 µM.

REFERENCES TO THE SUPPORTING INFORMATION

1. Mamo, J.; Insa, S.; Monclús, H.; Rodríguez-Roda, I.; Comas, J.; Barceló, D.; Farré, M. J., Fate of NDMA precursors through an MBR-NF pilot plant for urban wastewater reclamation and the effect of changing aeration conditions. *Water Res.* **2016,** *102*, 383-393.
2. Grebel, J. E.; Young, C. C.; Suffet, I. H., Solid-phase microextraction of N-nitrosamines. *J. Chromatogr. A* **2006,** *1117*, 11-18.
3. Bolton, J. R.; Mayor-Smith, I.; Linden, K. G., Rethinking the Concepts of Fluence (UV Dose) and Fluence Rate: The Importance of Photon-based Units – A Systemic Review. *Photochem. Photobiol.* **2015,** *91*, 1252-1262.
4. Daimon, M.; Masumura, A., Measurement of the refractive index of distilled water from the near-infrared region to the ultraviolet region. *Appl. Opt.* **2007,** *46*, 3811-3820.
5. Herrmann, H., On the photolysis of simple anions and neutral molecules as sources of O−/OH, SOx− and Cl in aqueous solution. *Phys. Chem. Chem. Phys.* **2007,** *9*, 3935-3964.
6. Sharpless, C. M.; Linden, K. G., Experimental and Model Comparisons of Low- and Medium-Pressure Hg Lamps for the Direct and H2O2 Assisted UV Photodegradation of N-Nitrosodimethylamine in Simulated Drinking Water. *Environ. Sci.Technol.* **2003,** *37*, 1933-1940.
7. Neta, P.; Huie, R. E.; Ross, A. B., Rate Constants for Reactions of Inorganic Radicals in Aqueous Solution. *J. Phys. Chem. Ref. Data* **1988,** *17*, 1027-1284.
8. Liang, C.; Su, H.-W., Identification of Sulfate and Hydroxyl Radicals in Thermally Activated Persulfate. *Ind. Eng. Chem. Res.* **2009,** *48*, 5558-5562.
9. Buxton, G. V.; Greenstock, C. L.; Helman, P. W.; Ross, A. B., Critical review of rate constants for reactions of hydrated electrons, hydrogen atoms and hydroxyl radicals (OH/O$^-$) in aqueous solution. *J. Phys. Chem.* **1988,** *17*, 513-886.
10. Das, T. N., Reactivity and Role of SO5•- Radical in Aqueous Medium Chain Oxidation of Sulfite to Sulfate and Atmospheric Sulfuric Acid Generation. *J.Phys. Chem. A* **2001,** *105*, 9142-9155.
11. Buxton, G. V.; Salmon, G. A.; Wood, N. D., A Pulse Radiolysis Study of the Chemistry of Oxysulphur Radicals in Aqueous Solution. In: *Physico-Chemical Behaviour of Atmospheric Pollutants: Air Pollution Research Reports.*, Restelli, G.; Angeletti, G., Eds. Springer Netherlands: Dordrecht, **1990**; 245-250.
12. Wols, B. A.; Hofman-Caris, C. H. M., Review of photochemical reaction constants of organic micropollutants required for UV advanced oxidation processes in water. *Water Res.* **2012,** *46*, 2815-2827.
13. Peyton, G. R., The free-radical chemistry of persulfate-based total organic carbon analyzers. *Mar. Chem.* **1993,** *41*, 91-103.
14. Yang, Y.; Pignatello, J. J.; Ma, J.; Mitch, W. A., Comparison of Halide Impacts on the Efficiency of Contaminant Degradation by Sulfate and Hydroxyl Radical-Based Advanced Oxidation Processes (AOPs). *Environ. Sci.Technol.* **2014,** *48*, 2344-2351.
15. Clifton, C. L.; Huie, R. E., Rate constants for hydrogen abstraction reactions of the sulfate radical, SO4−. Alcohols. *Int. J. Chem. Kinet.* **1989,** *21*, 677-687.
16. Huie, R. E.; Clifton, C. L., Temperature dependence of the rate constants for reactions of the sulfate radical, SO4-, with anions. *J. Phys. Chem.* **1990,** *94*, 8561-8567.
17. Crittenden, J. C.; Hu, S.; Hand, D. W.; Green, S. A., A kinetic model for H2O2/UV process in a completely mixed batch reactor. *Water Res.***1999,** *33*, 2315-2328.
18. Buxton, G. V.; Bydder, M.; Arthur Salmon, G.; Williams, J. E., The reactivity of chlorine atoms in aqueous solution. Part III. The reactions of Cl[round bullet, filled] with solutes. *Phys. Chem. Chem. Phys.* **2000,** *2*, 237-245.
19. Matthew, B. M.; Anastasio, C., A chemical probe technique for the determination of reactive halogen species in aqueous solution: Part 1 – bromide solutions. *Atmos. Chem. Phys.* **2006,** *6*, 2423-2437.
20. Buxton, G. V.; Bydder, M.; Arthur Salmon, G., Reactivity of chlorine atoms in aqueous solution Part 1The equilibrium ClMNsbd+Cl-Cl2. *J. Chem. Soc. Faraday T.* **1998,** *94*, 653-657.

21. Kläning, U. K.; Wolff, T., Laser Flash Photolysis of HClO, ClO−, HBrO, and BrO− in Aqueous Solution. Reactions of Cl- and Br-Atoms. *Berich.Bunsen. Phys.Chem.* **1985,** *89*, 243-245.
22. Yu, X.-Y.; Barker, J. R., Hydrogen Peroxide Photolysis in Acidic Aqueous Solutions Containing Chloride Ions. I. Chemical Mechanism. *J. Phys. Chem. A* **2003,** *107*, 1313-1324.
23. Yu, X.-Y.; Bao, Z.-C.; Barker, J. R., Free Radical Reactions Involving $Cl^{\bullet}$, $Cl_2^{-\bullet}$, and $SO_4^{-\bullet}$ in the 248 nm Photolysis of Aqueous Solutions Containing $S_2O_8^{2-}$ and Cl. *J. Phys. Chem. A* **2004,** *108*, 295-308.
24. Jayson, G. G.; Parsons, B. J.; Swallow, A. J., Some simple, highly reactive, inorganic chlorine derivatives in aqueous solution. Their formation using pulses of radiation and their role in the mechanism of the Fricke dosimeter. *J. Chem. Soc. Faraday T.* **1973,** *69*, 1597-1607.
25. Wagner, I.; Karthäuser, J.; Strehlow, H., On the Decay of the Dichloride Anion Cl−2 in Aqueous Solution. *Berich.Bunsen. Phys.Chem.* **1986,** *90*, 861-867.
26. Zehavi, D.; Rabani, J., Oxidation of aqueous bromide ions by hydroxyl radicals. Pulse radiolytic investigation. *J. Phys. Chem.* **1972,** *76*, 312-319.
27. Grigor'ev, A. E.; Makarov, I. E.; Pikaev, A. K., Formation of Cl_2^- in the bulk solution during the radiolysis of concentrated aqueous solutions of chlorides. *High Energy Chem.* **1987**, *21*, 99-102.
28. Buxton, G. V.; Bydder, M.; Arthur Salmon, G.; Williams, J. E., The reactivity of chlorine atoms in aqueous solution. Part III. The reactions of Cl• with solutes. *Phys. Chem. Chem. Phys.* **2000,** *2*, 237-245.